Integrated simulations of fast ignition of inertial fusion targets
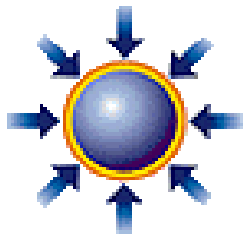
Javier Honrubia

School of Aerospace Engineering
Technical University of Madrid, Spain
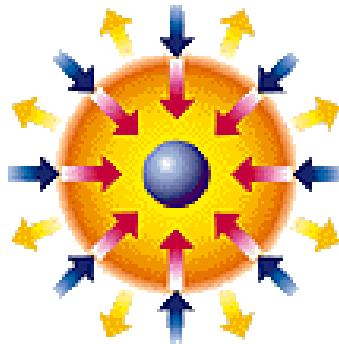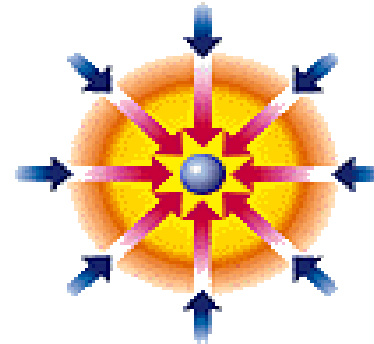
Inertial Confinement Fusion

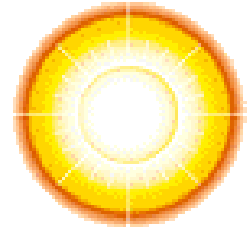1-2 mm radius
10^{14}-10^{15} W/cm^2
a few ns

Lasers or X-rays
symmetrically
irradiate pellet

Hot plasma expands into
vacuum causing shell to
implode with high velocity

Material is
compressed to
~1000 gcm^{-3}

Hot spark formed at
the centre of the fuel
by convergence of
accurately timed
shock waves
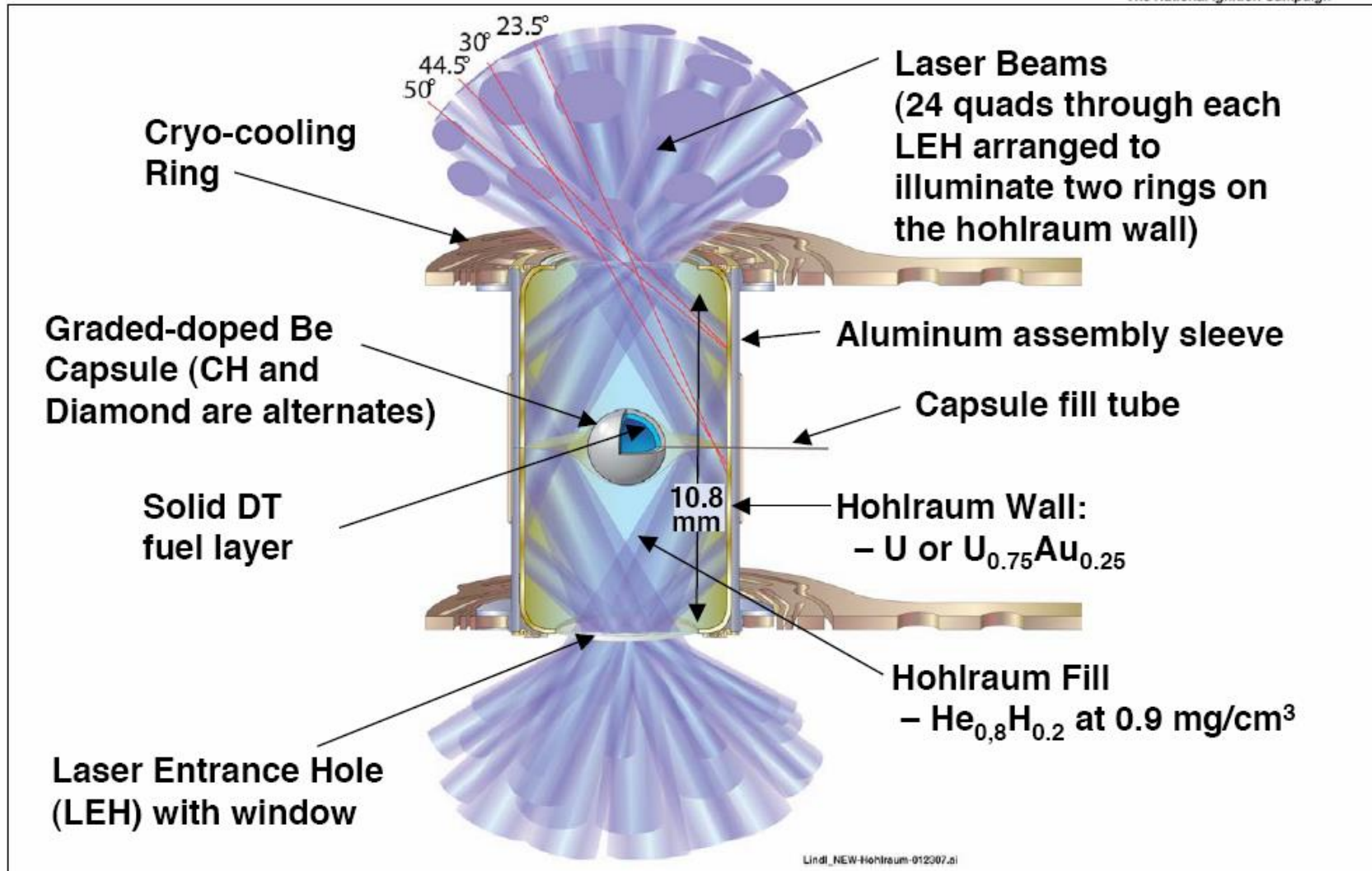
National Ignition Facility (NIF)

NIF Laser System

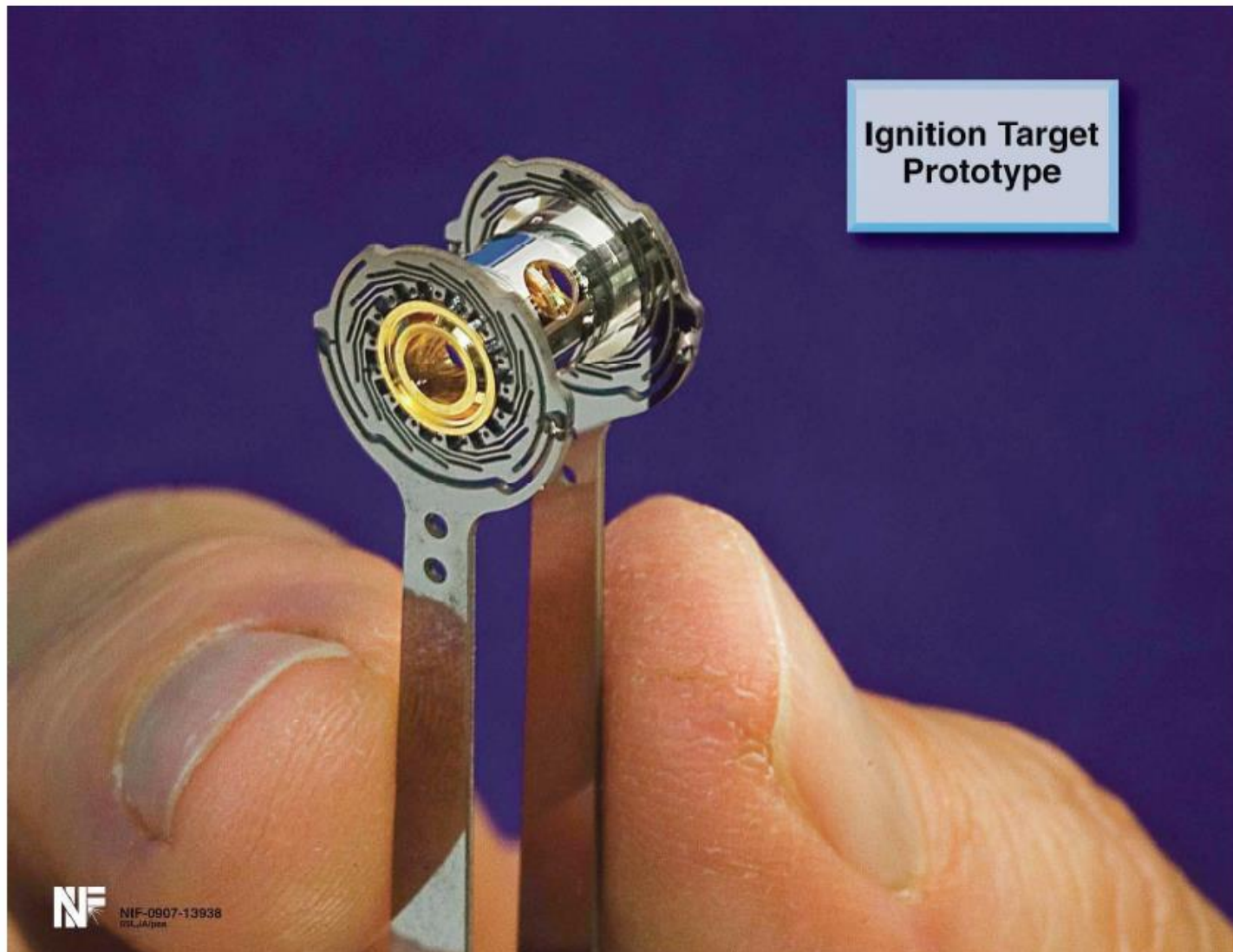- 192 Beams
- Frequency tripled Nd glass
- Energy   1.8 MJ
- Power   500 TW
- Wavelength   351 nm

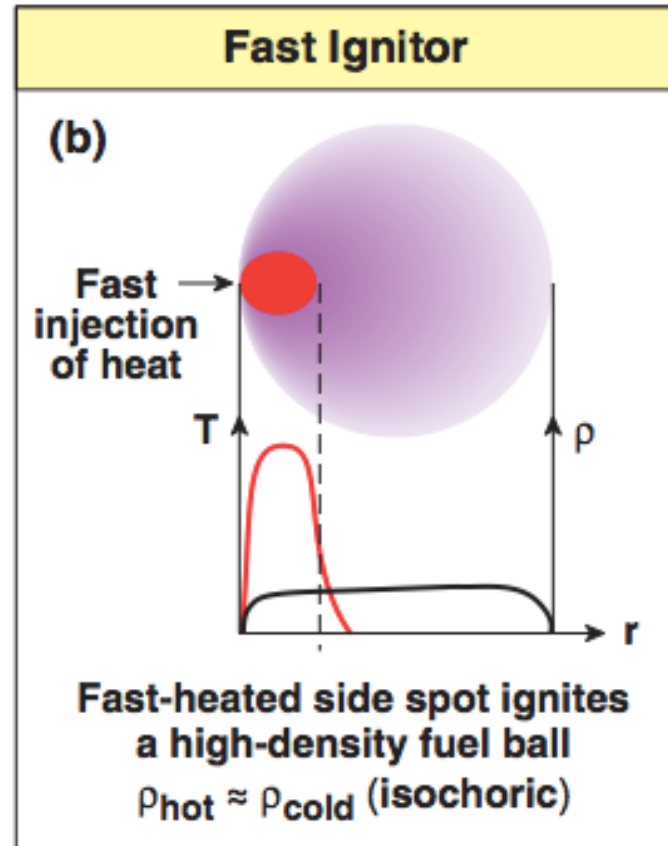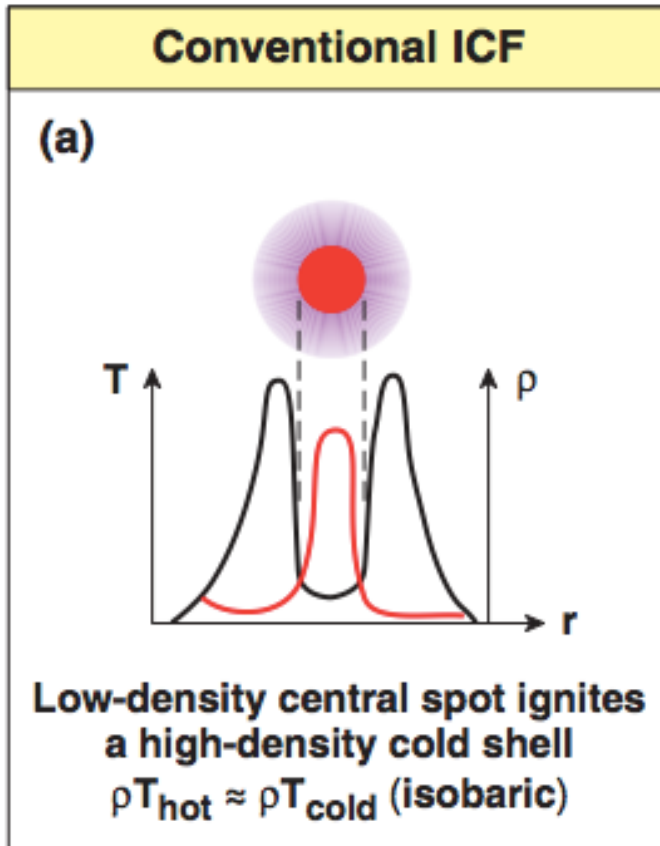NIF is 50 times more energetic than any previous laser

07EIM/mfm • NIF-2009-Aerial PERFORMANCE-s1 L2

The NIF point design has a graded-doped, beryllium capsule in a hohlraum driven at 285 eV

30° 23.5°
44.5°
50°

Laser Beams
(24 quads through each LEH arranged to illuminate two rings on the hohlraum wall)

Cryo-cooling Ring

Graded-doped Be Capsule (CH and Diamond are alternates)

Aluminum assembly sleeve

Capsule fill tube

Solid DT fuel layer

10.8 mm

Hohlraum Wall:
– U or $U_{0.75}Au_{0.25}$

Hohlraum Fill
– $He_{0.8}H_{0.2}$ at 0.9 mg/cm^3

Laser Entrance Hole (LEH) with window

Lindl_NEW-Hohlraum-012307.ai

Precision targets being developed for the NIF meet the ignition target requirements

Ignition Target Prototype

Central ignition vs. Fast ignition

Conventional ICF

(a)

Low-density central spot ignites a high-density cold shell
$\rho T_{hot} \approx \rho T_{cold}$ (isobaric)

Fast Ignitor

(b)

Fast injection of heat

Fast-heated side spot ignites a high-density fuel ball
$\rho_{hot} \approx \rho_{cold}$ (isochoric)

Fast ignition can be achieved with lower drive energies

➢ Separation between implosion and ignition phases.

Direct drive FI ($\rho r = 3gcm^{-2}$)

Direct drive FI ($\rho r = 1.5gcm^{-2}$)

300g/cc
92kJ
4×10^{19}

100

Fast Ignition

200 g/cc,
200 kJ,
2.5×10^{19}

Target gain

10

150 g/cc,
330 kJ,
1.8×10^{19}

1
0.1

1000-MJ yield

100-MJ yield

10-MJ yield

NIF

NIF Point Designs

Direct Drive

Indirect drive

$v = 4 \times 10^7$

$v = 3 \times 10^7$

Driver energy (MJ)

10
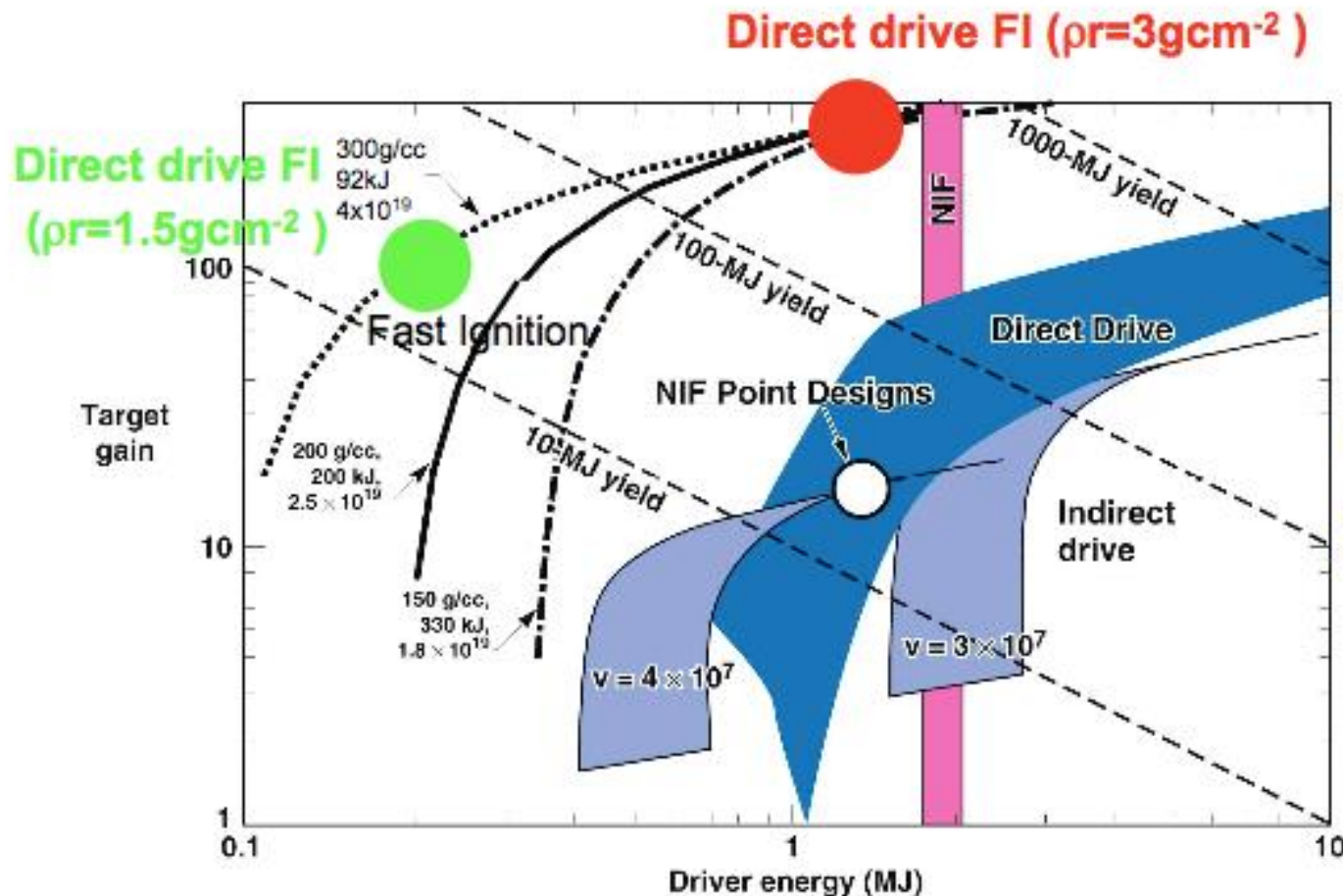
M H Key et al. J. Fus. Energy 17, 231, (1998)

Fast ignition schemes
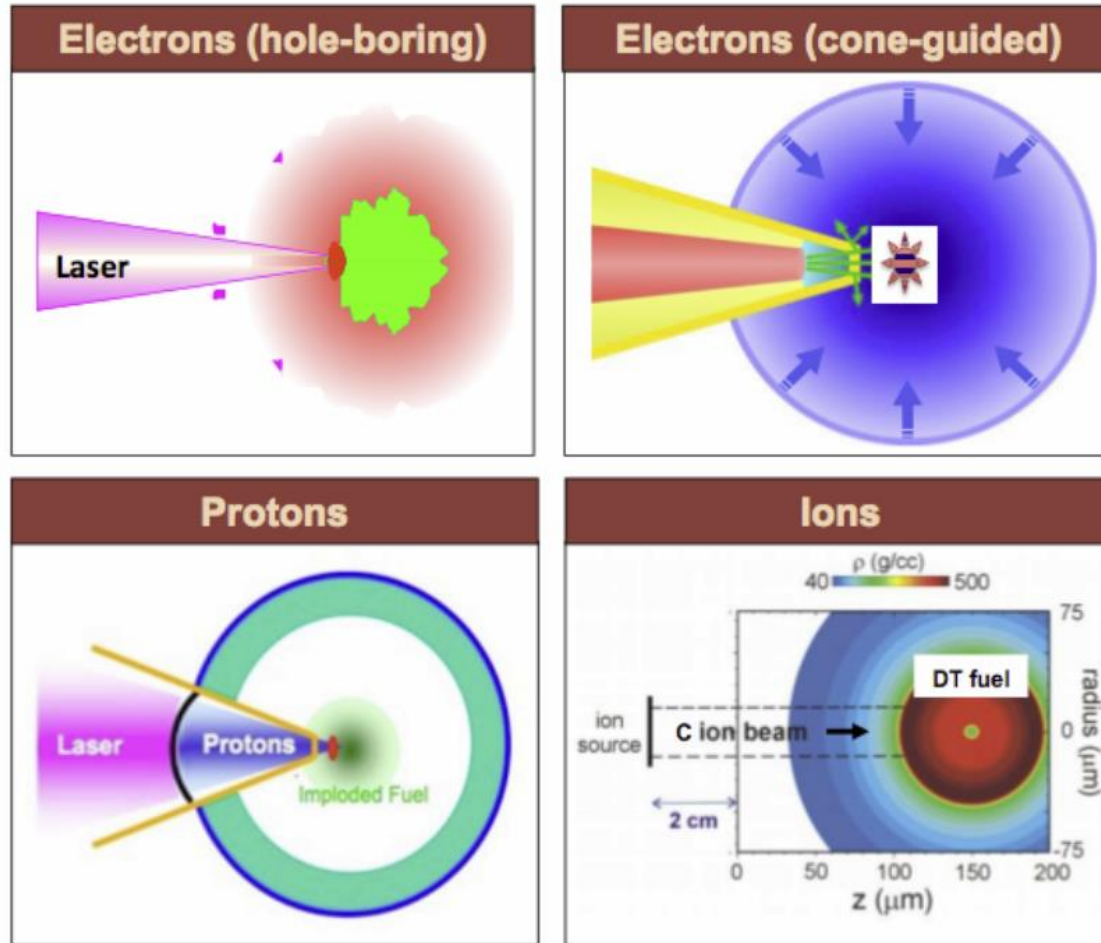
Our simulation work

- ➢ The research projects carried out on Marenostrum and Magerit HPC have been focused to analyse alternative ignition schemes of inertial confinement fusion capsules with the aim of lowering the ignition threshold.

- ➢ The following schemes have been explored so far:

  - **Electron-driven fast ignition** of inertial fusion targets, where an electron jet is generated by the interaction of an ultra-high intensity (UHI) laser with the cone tip. The electrons deposit their energy in the compressed core triggering the fusion reaction.

  - **Ion-driven fast ignition** the same but driven by UHI laser-accelerated ions.

  - **Magnetized inertial fusion targets**. Just started.

- ➢ The simulation codes used have been as follows:

  - The Particle-In-Cell (PIC) codes **PICLS** [Sentoku & Kemp, *JCP* **227**, 6846 (2008)] and **EPOCH** [Arber *et al.*, *PPCF* **57**, 113001 (2015)].

  - The hybrid code **PETRA** [Honrubia *et al.*, *Phys. Plasmas* **12**, 052708 (2005)].

  - The magneto-hydrodynamic code **ATHENA** [Stone & Gardiner, *J. Comput. Phys.* **205,** 209 (2005)].

The first integrated FI experiment was very successful

Kodama *et al.*, *Nature* **412**, 798 (2001) and Kodama *et al.*, Nature **418**, 933 (2002)

GEKKO laser
9 beams, 0.53 μm, 1.2 kJ / 1ns

0.5 PW
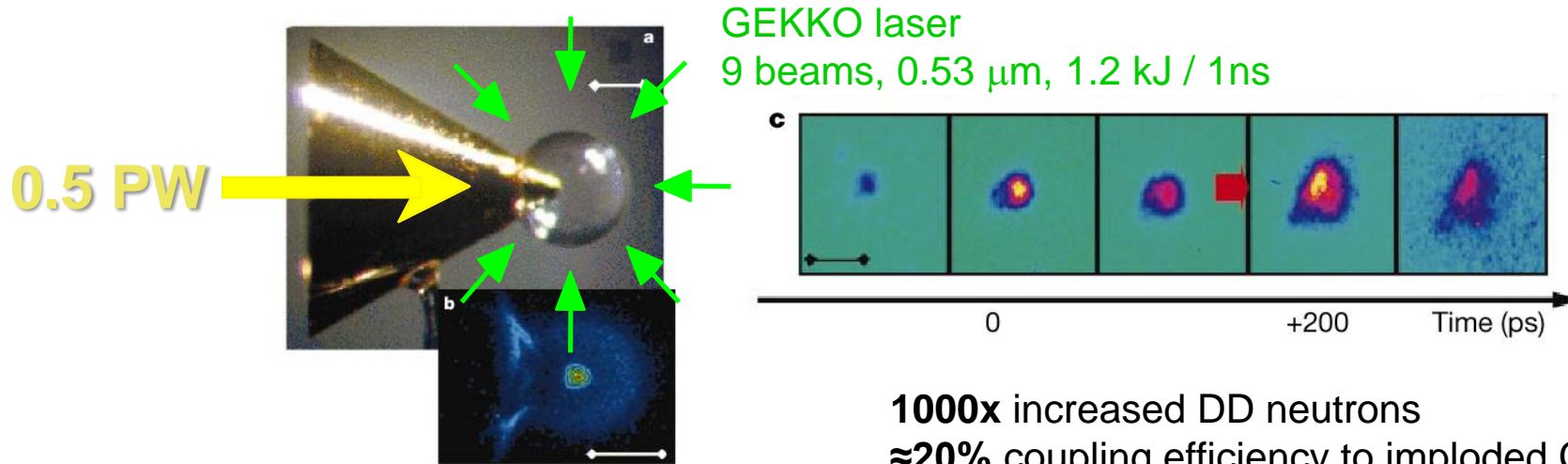
1000x increased DD neutrons
≈20% coupling efficiency to imploded CD
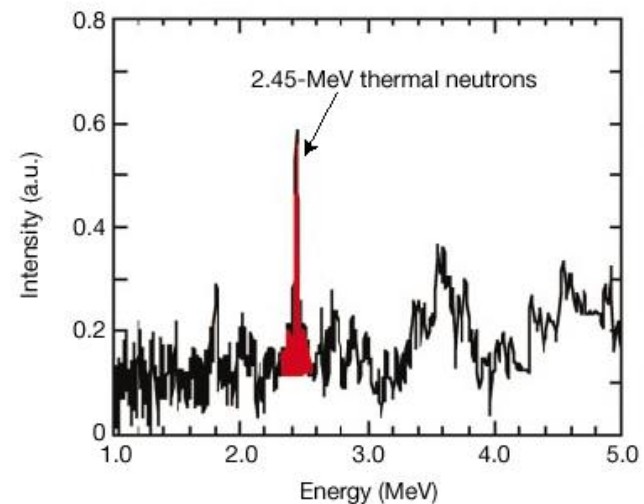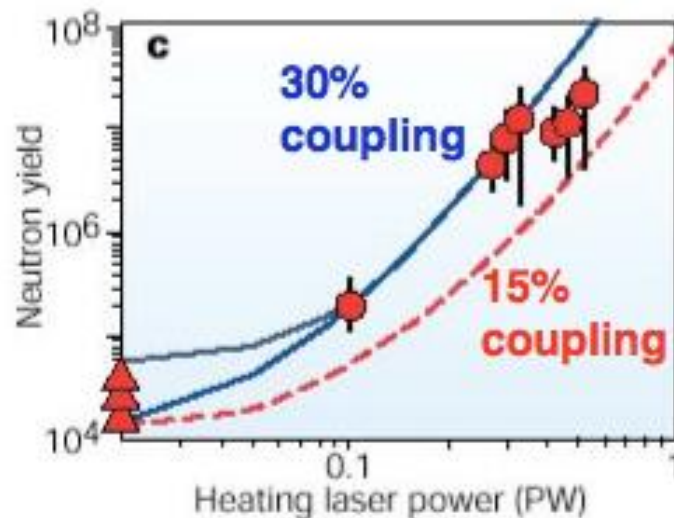
Beam collimation by density effects:
Experiment on fast electron transport in high density plasmas

Experimental setup

Experiment carried out at RAL

Pérez, Honrubia *et al.*, Phys Rev. Lett. **107**, 065004 (2011)

4 long pulse beams

1ns – 40-50J each at $2\omega_0$
160µm focal spots (1/e)

Ni foil to produce
the hot electrons

Target description

Polyimide shell
1.1g/cc, 20µm thick

CH foam
ρ_m=0.1, 0.3 or 1g/cc

200µm long

Gold shield

Copper foil

Short pulse beam

12 ps – 160 J at ω_0
20µm FWHM spot
4×10^{18} W/cm²

foam diameter = 180µm

Polyimide hollow cylinder

containing CH foam of 3 ≠ densities:
0.1, 0.3 and 1g/cc

CH covered
Au cylinder

Polyimide
cylinder

CH covered
Cu foil

Ni foil

200 µm

Foams polymerized by W. Nazarov (Univ. St. Andrews)
Targets assembled at RAL (Ch. Spindloe *et al.*)
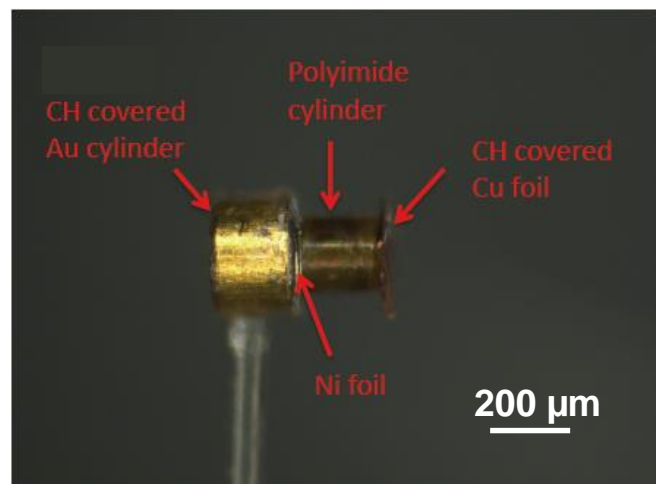
Simulation strategy

➢ **3-D radiation-hydrodynamics** for the cylinder implosion and compression.

➢ **2D PIC** simulations to characterize the fast electrons generated by the short pulse laser.

➢ **Hybrid** simulations for simulation of fast electron transport in the compressed cylinder including self-generated electromagnetic fields.

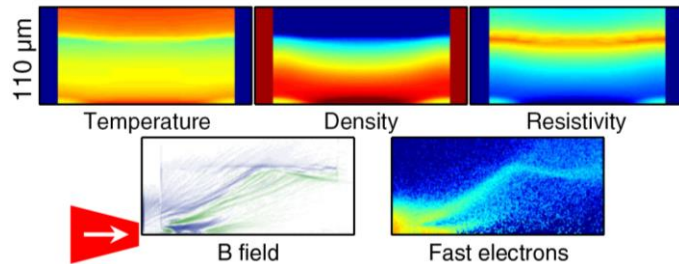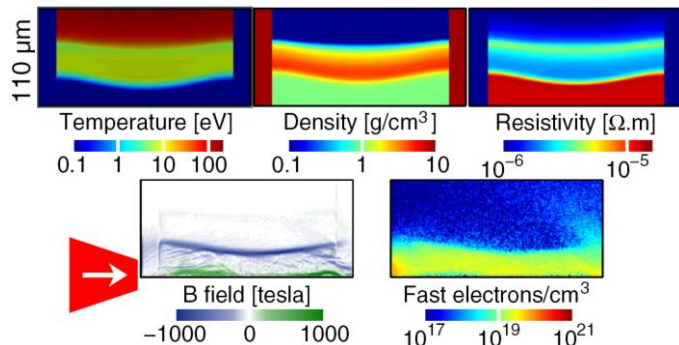### 3-D hydrodynamic simulations of target compression

1 g/cm^3 foam.
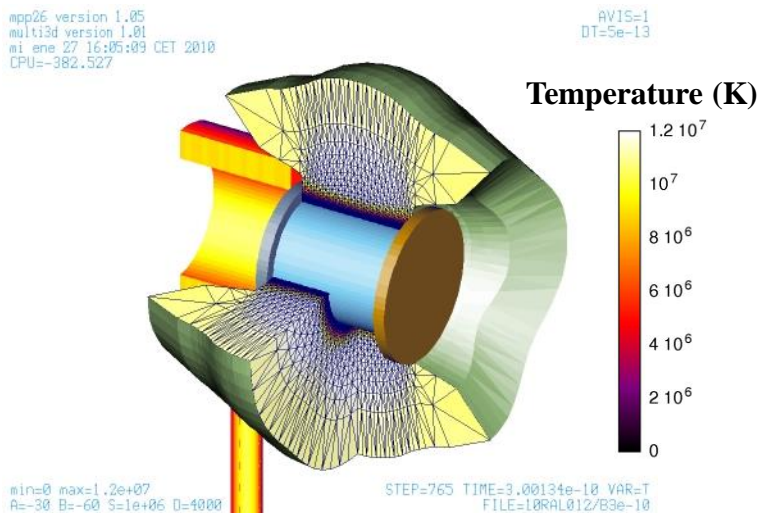
0.1 g/cm^3 foam.
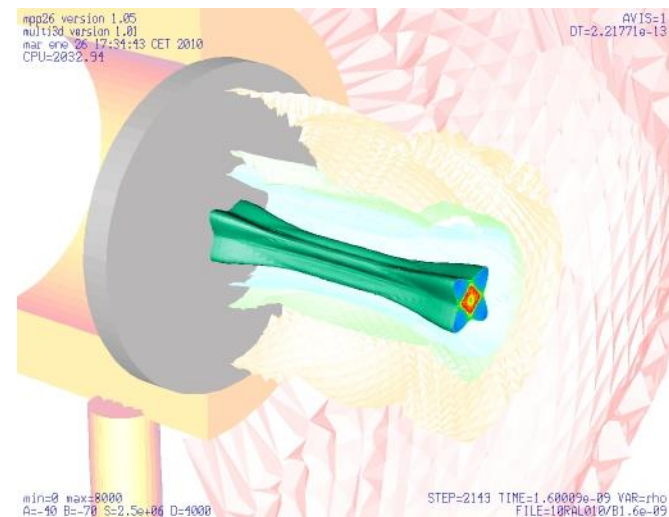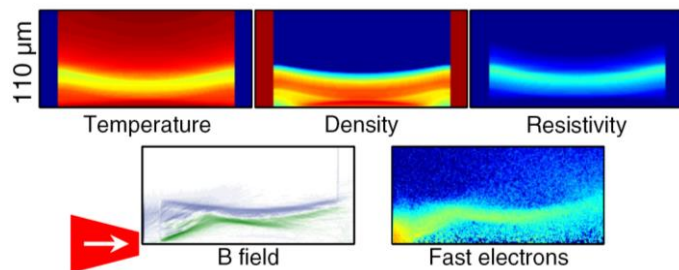
First experimental evidence of e-beam collimation

Pérez *et al.*, Phys. Rev. Lett. **107**, 065004 (2011)

Integrated simulations
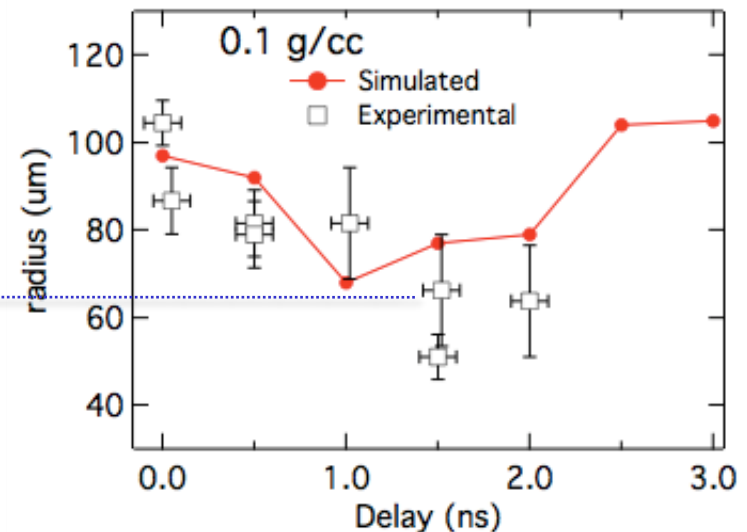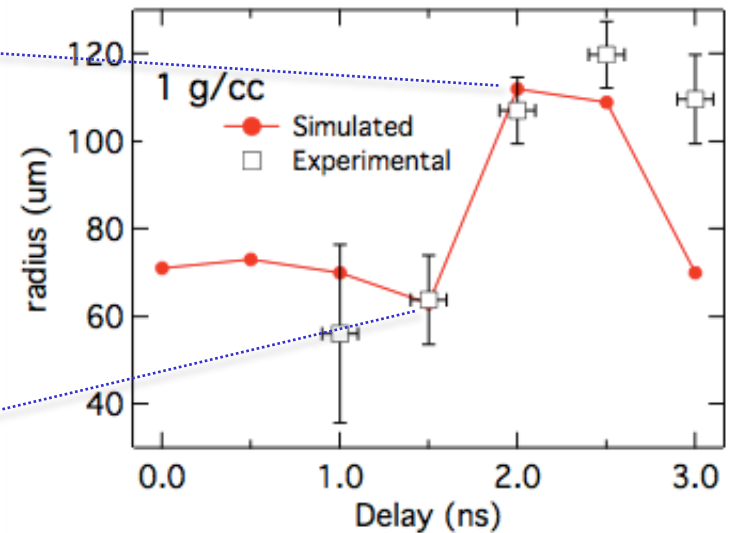# of ignition-scale targets

PIC simulations of electron acceleration in a double cone

➢ Cone parameters: $\theta = 15^0$, $d_{int} = 10$ μm, $d_{ext}=20$ μm, $n_e = 80$ n_c and $Z^* = 40$ [Debayle, Honrubia *et al.*, Phys. Rev. E **82**, 036405 (2010)].

➢ Numerical parameters: $\Delta x = \Delta y = \lambda/50$, 40 electron/cell.

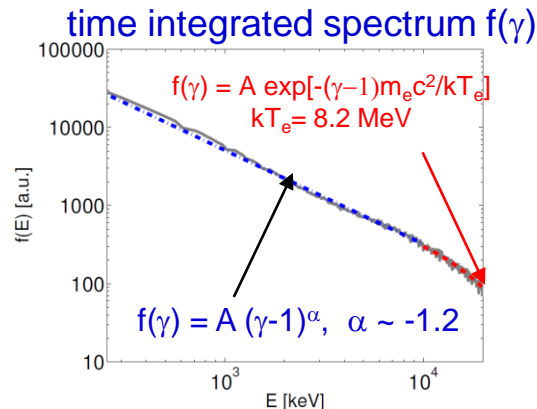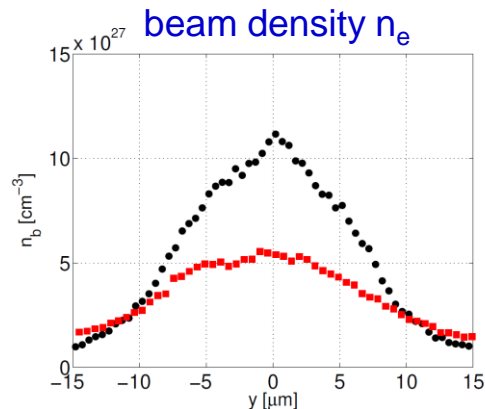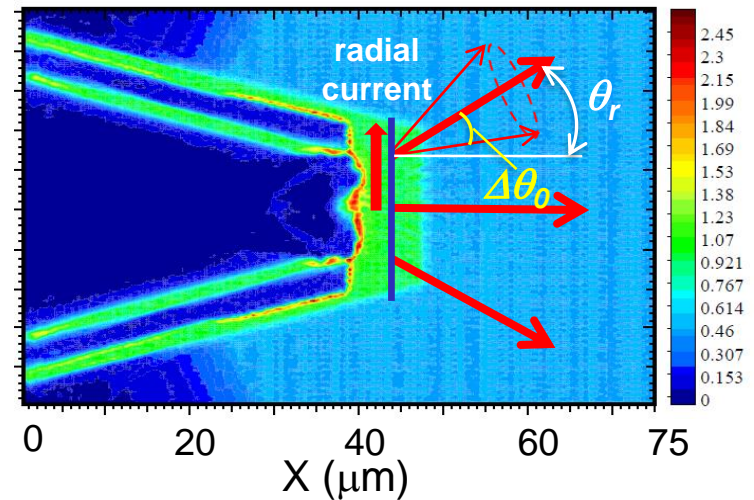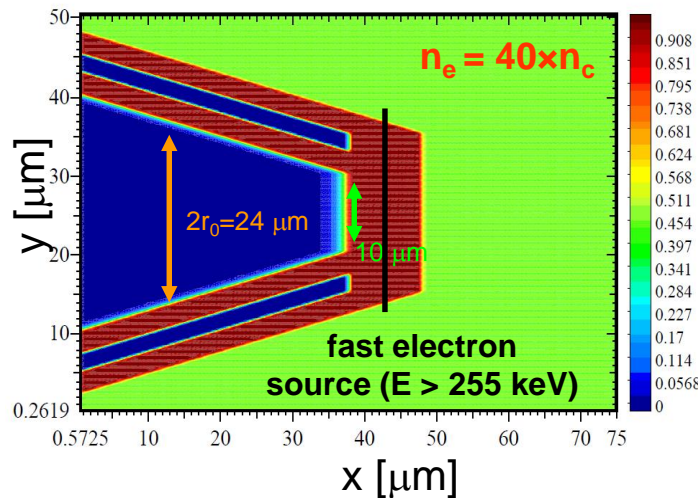➢ 10 million cells, 400 million particles.

laser beam

2x10²⁰ W/cm²

p - polarized

$\lambda = 1$ μm

pulse length 1 ps

focal spot = 24 μm

$n_e = 40 \times n_c$

$2r_0 = 24$ μm

10 μm

fast electron source (E > 255 keV)

x [μm]

y [μm]

radial current

θ_r

$\Delta\theta_0$

X (μm)

beam density n_e

n_b [cm⁻³]

y [μm]

time integrated spectrum f(γ)

$f(\gamma) = A \exp[-(\gamma-1)m_ec^2/kT_e]$
$kT_e = 8.2$ MeV

$f(\gamma) = A (\gamma-1)^\alpha$, $\alpha \sim -1.2$

f(E) [a.u.]

E [keV]

$$f(\theta) = A \exp\left(-\left[\frac{\theta - \theta_r(y,t)}{\Delta\theta_0(y,t)}\right]^2\right)$$

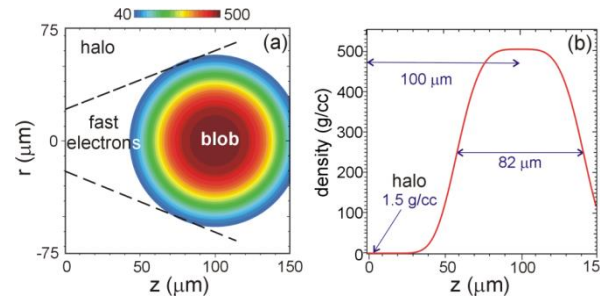# Simulations with 'standard' injection

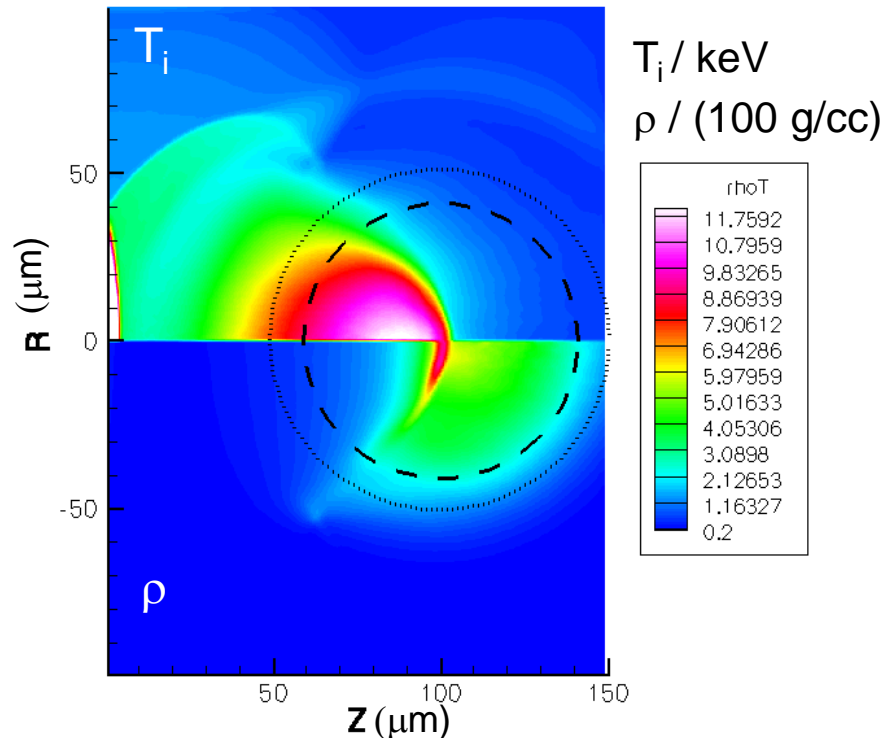**electron injection without radial drift**

E_{ig} = 36 kJ
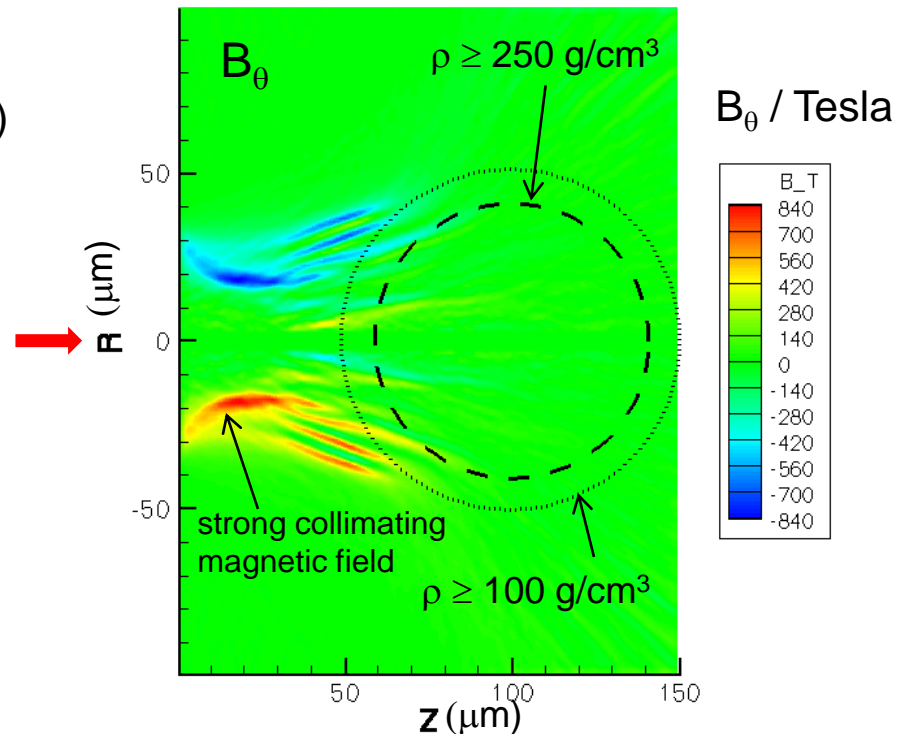$\langle E \rangle$ = 1.6 MeV
$\theta_{HWHM} = \Delta\theta_0$ = 35°

Honrubia & Meyer-ter-Vehn, Plasma Phys. Control. Fusion **51**, 014008 (2009)
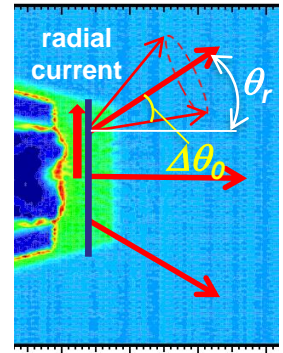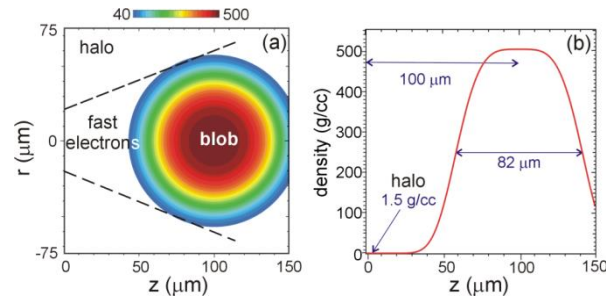
Ion temperature and density

T_i

T_i / keV
ρ / (100 g/cc)

ρ

Resistive magnetic field

B_θ

B_θ / Tesla

$\rho \geq 250$ g/cm^3

strong collimating magnetic field

$\rho \geq 100$ g/cm^3

Simulations with 'PIC' injection ($\theta_r \neq 0$)

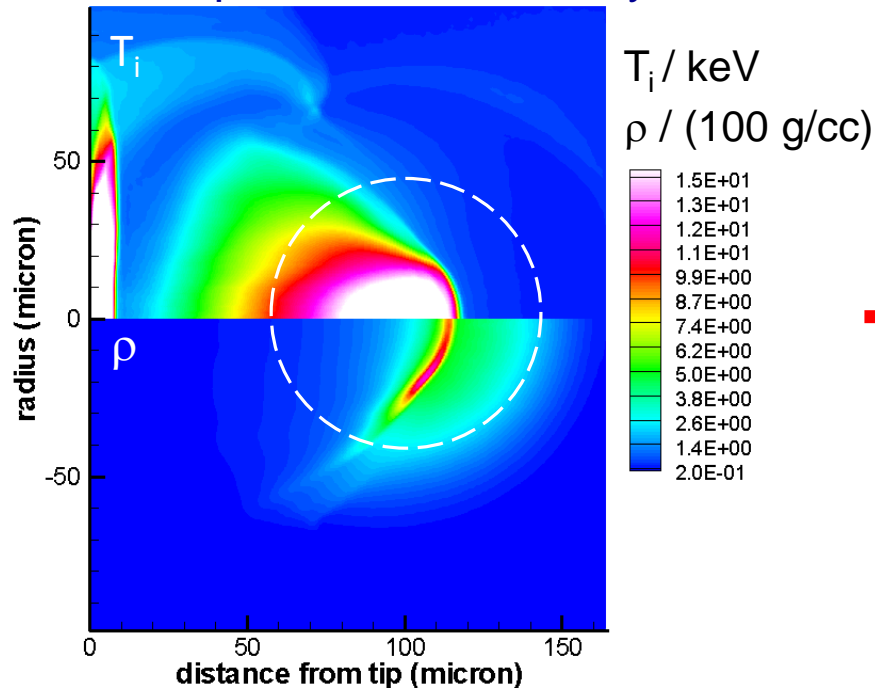**electron injection with radial drift**

E_{ig} = 40 kJ
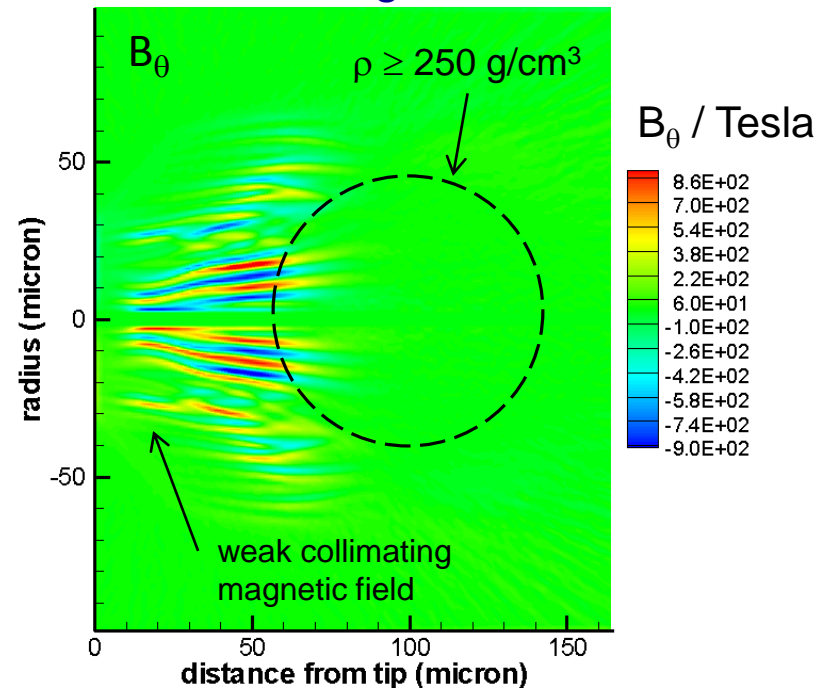$\langle E \rangle$ = 1 MeV
$\Delta\theta_0$ = 22°, θ_r = 20°

Debayle, Honrubia *et al.*, Plasma Phys. Control. Fusion **52**, 124024 (2010)

Ion temperature and density

T_i / keV
ρ / (100 g/cc)

1.5E+01
1.3E+01
1.2E+01
1.1E+01
9.9E+00
8.7E+00
7.4E+00
6.2E+00
5.0E+00
3.8E+00
2.6E+00
1.4E+00
2.0E-01

Resistive magnetic field

$\rho \geq 250$ g/cm³

B_θ / Tesla

8.6E+02
7.0E+02
5.4E+02
3.8E+02
2.2E+02
6.0E+01
-1.0E+02
-2.6E+02
-4.2E+02
-5.8E+02
-7.4E+02
-9.0E+02

weak collimating magnetic field

Experimental evidence of fast electron collimation by external magnetic fields

PS shell

Ta

LFEX

GXII

e⁻

X ray

e⁻

X ray

e⁻

X ray

1 mm
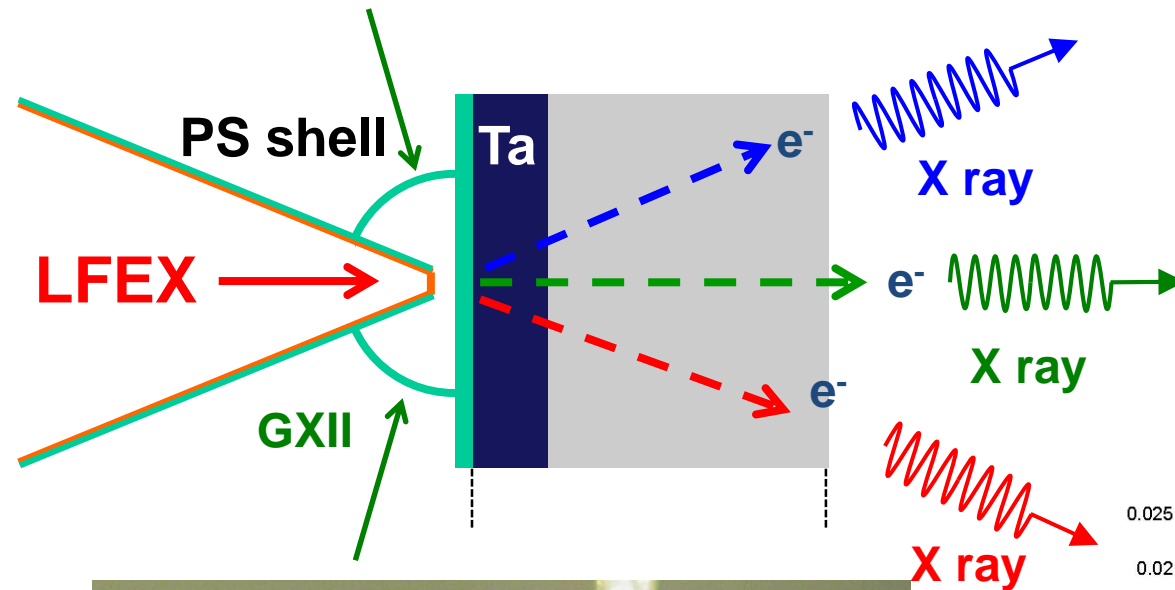
Fujioka *et al.*, Phys. Rev. E **91**, 063102 (2015)

Simulations by H. Nagatomo

ρ

T

Time= 2.570

Density
100
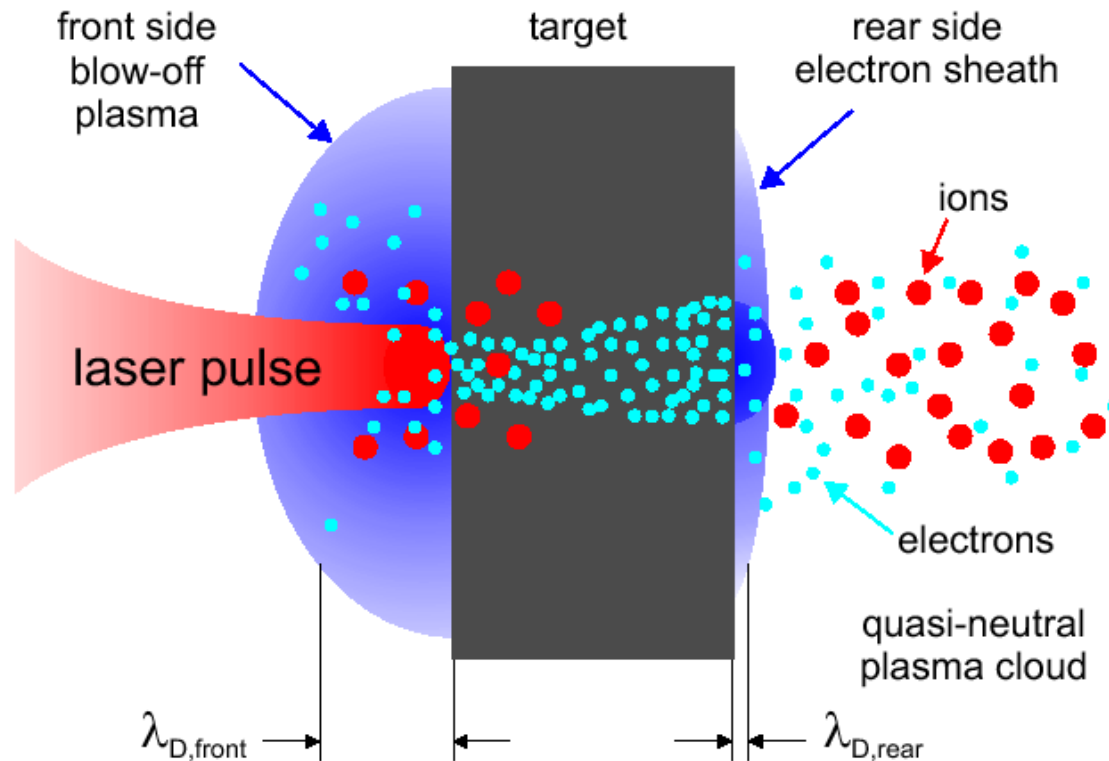10
1
0.1
0.01

Te
1
0.1
0.01
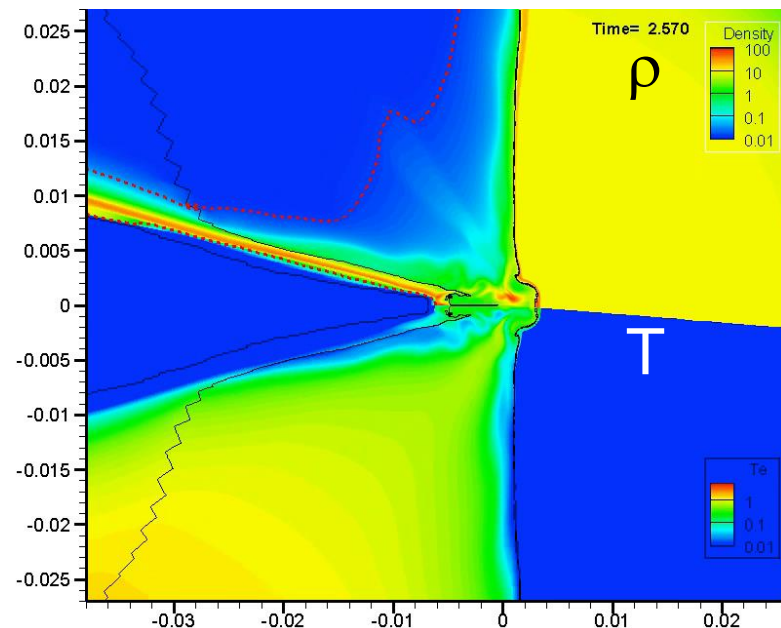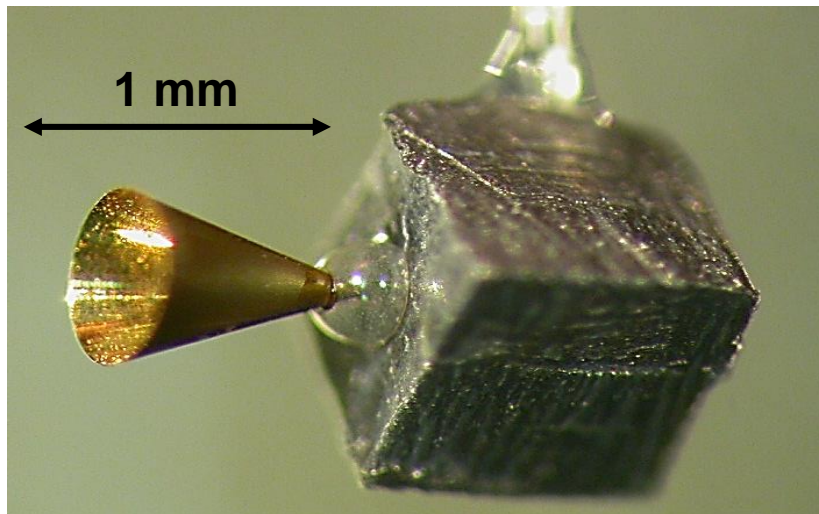
Spectrum, angular distribution, image of x-rays are measured.

Ion-driven fast ignition

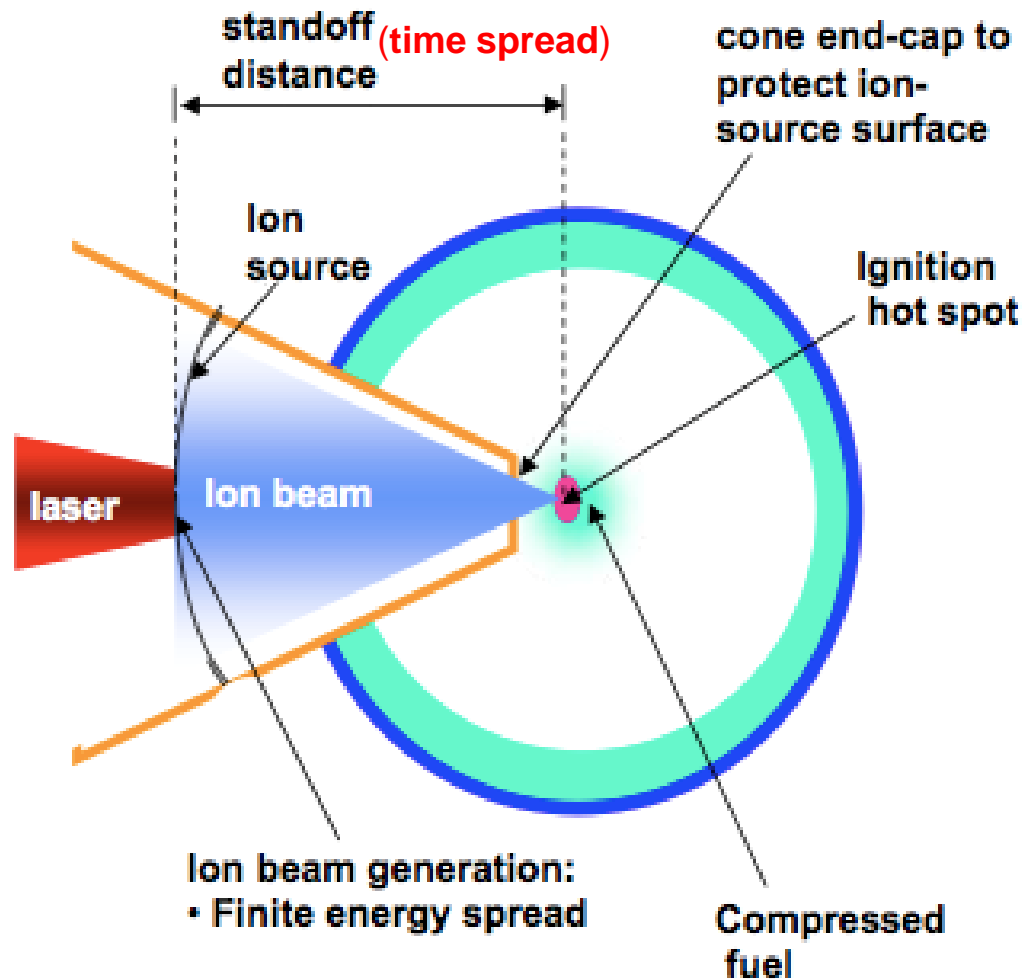# Generation extremely bright ion beams by the TNSA scheme

Target Normal Sheath Acceleration scheme [Snavely *et al.*, PRL **85**, 2945 (2000)]
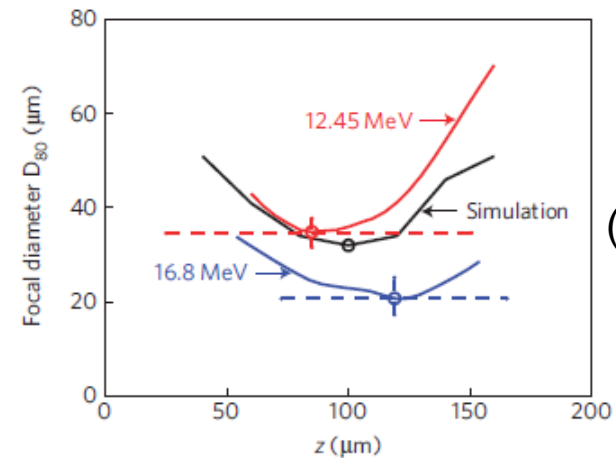

Fluid model: P. Mora, PRL **90**, 185002 (2003)
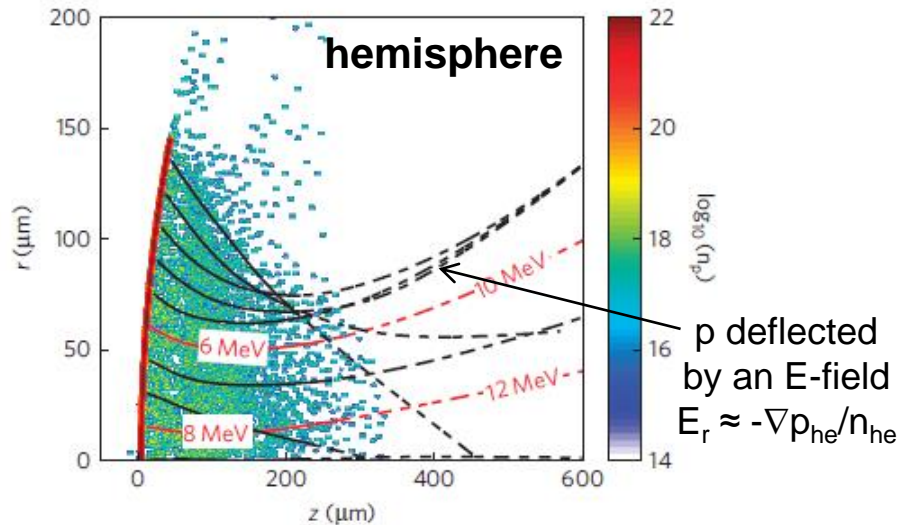
$$E_{\max} = 2T_{hot}\left[\ln\left(t + (t^2 + 1)^{1/2}\right)\right]^2 \quad ; \quad t = \frac{w_{pi}t_{acc}}{\left[2\exp(1)\right]^{1/2}} \quad ; \quad w_{pi} = \left(\frac{Z_i e^2 n_{e0}}{e_0 m_i}\right)^{1/2}$$
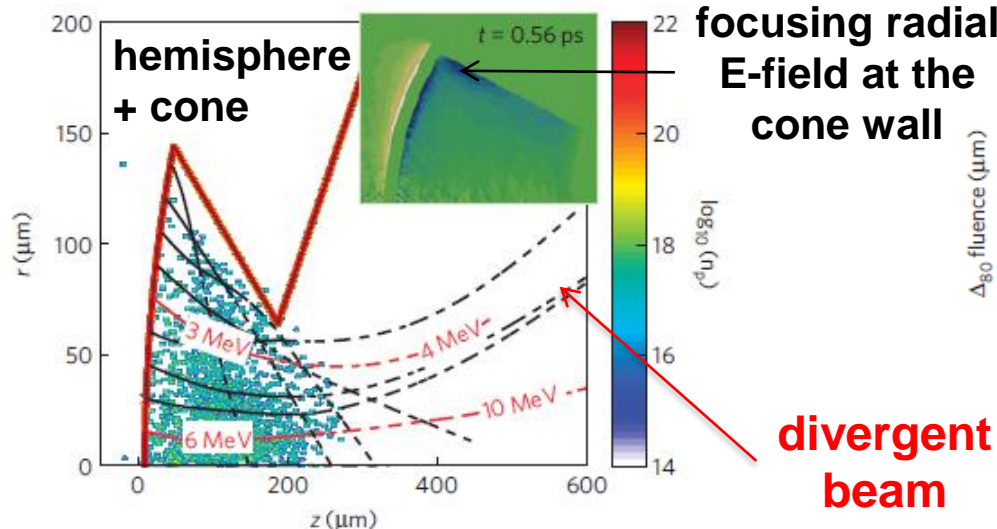
"classical" proton FI scheme

Proton focusing in cone-targets has been demonstrated experimentally

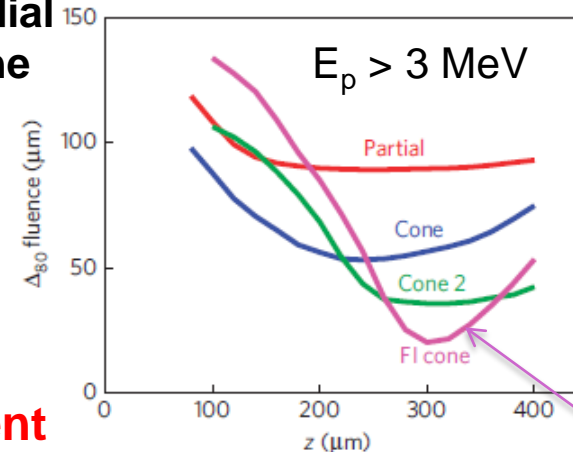Bartal *et al., Nature Phys.* **8**, 139 (2012), Foord *et al., Phys. Plasmas* **19**, 056702 (2012), Qiao *et al., Phys. Rev. E* **87**, 013108 (2013)

hemisphere

p deflected by an E-field $E_r \approx -\nabla p_{he}/n_{he}$

laser

D_{80} (> 9 MeV)

hemisphere + cone

focusing radial E-field at the cone wall

divergent beam

E_p > 3 MeV

Fluence diameter

Expanded hot e source

Au cone 20 μm !

PIC simulation data

Open PIC code **EPOCH-2D** [Arber *et al.*, *PPCF* **57**, 113001 (2015)].

Target [Honrubia, Morace and Murakami, *MRE* **2**, 28-36 (2017); submitted to Phys. Plasmas (2017)].

  Length (x) = 130 μm, width (y) = 90 μm.

  Pre-plasma: exponential profile with a scale-length = 2 μm.

  Grid: 15 million cells, 600 million particles.

Laser

  Wavelength λ = 1.06 μm.

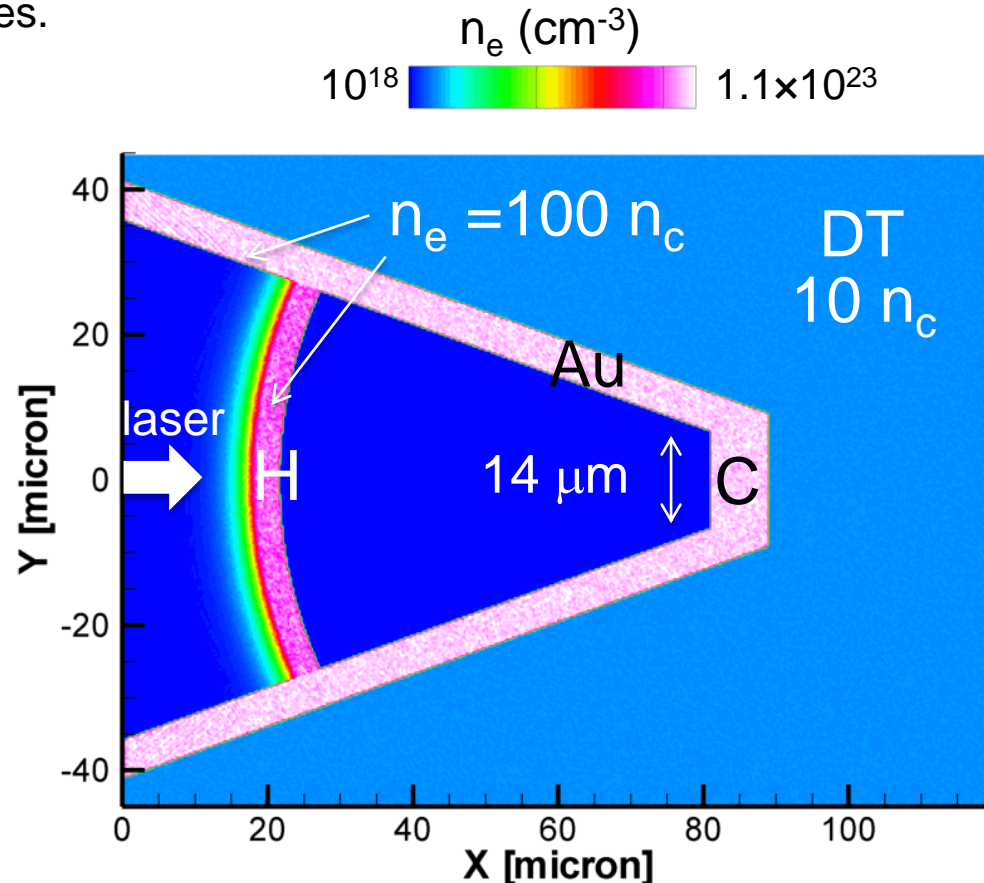 Peak laser intensity I_0 = 10^{20} W/cm^2.

  Spatial profile: Super-Gaussian,
      FWHM = 55 μm.

  Temporal profile: Gaussian,
      FWHM = from 1 to 0.35 ps.

Boundary conditions for particles and fields

  x : laser and thermal

  y : periodic

n_e (cm^{-3})

10^{18} 1.1×10^{23}

n_e = 100 n_c

DT
10 n_c

Au

laser

H

14 μm   C

Proton beam defocusing by the B-field

- B-field generation at the cone wall by a surface current [Zou *et al.*, *Phys. Plasmas* **22**, 063103 (2015)].

- B-field is dragged by the quasi-neutral plasma of protons + co-moving electrons.

- B-field is amplified and compressed at the cone tip.

- The polarity of the B-field is such that protons are de-collimated, hollowing or even breaking the proton beam.
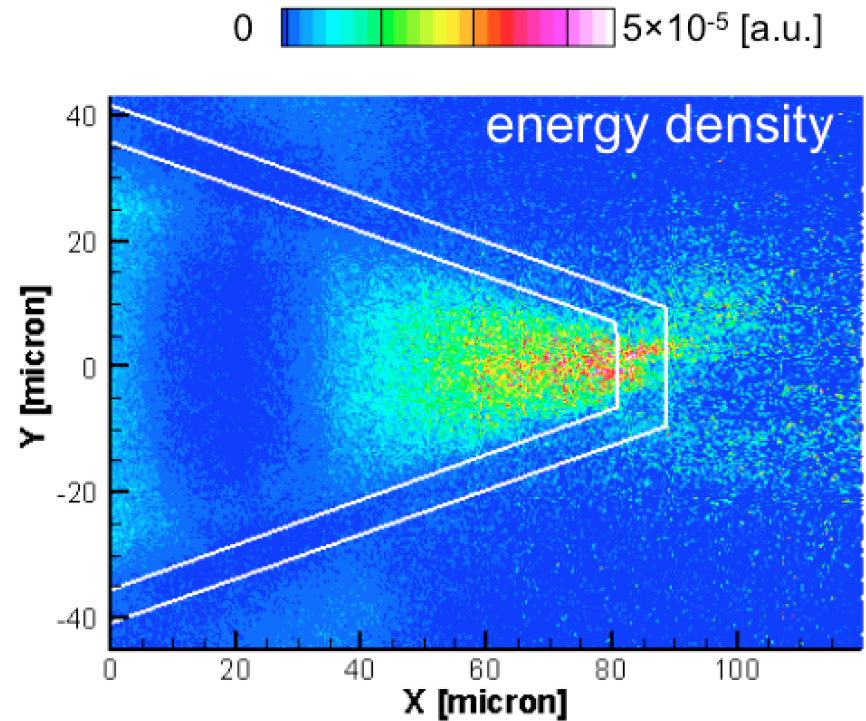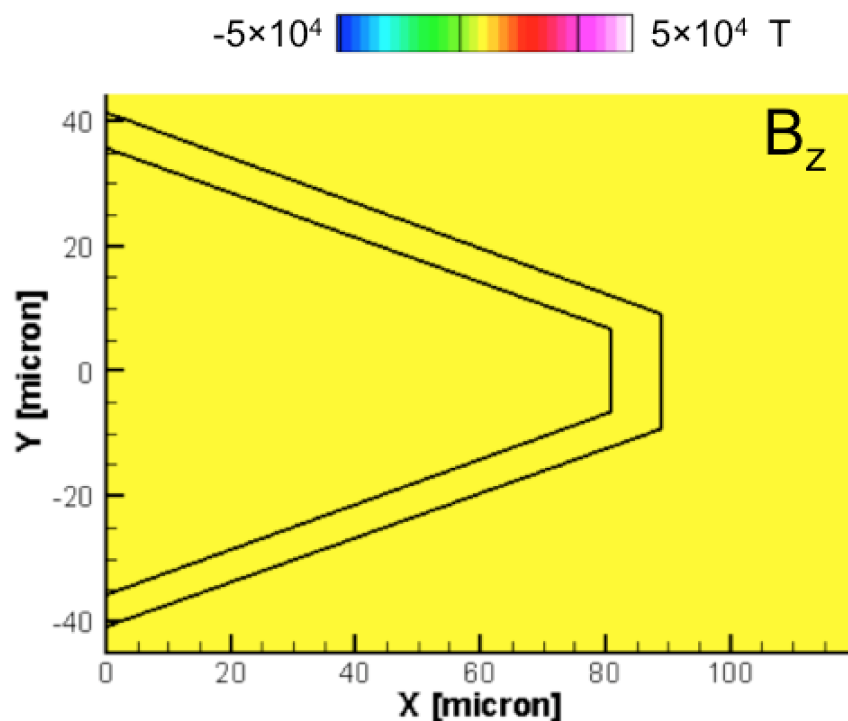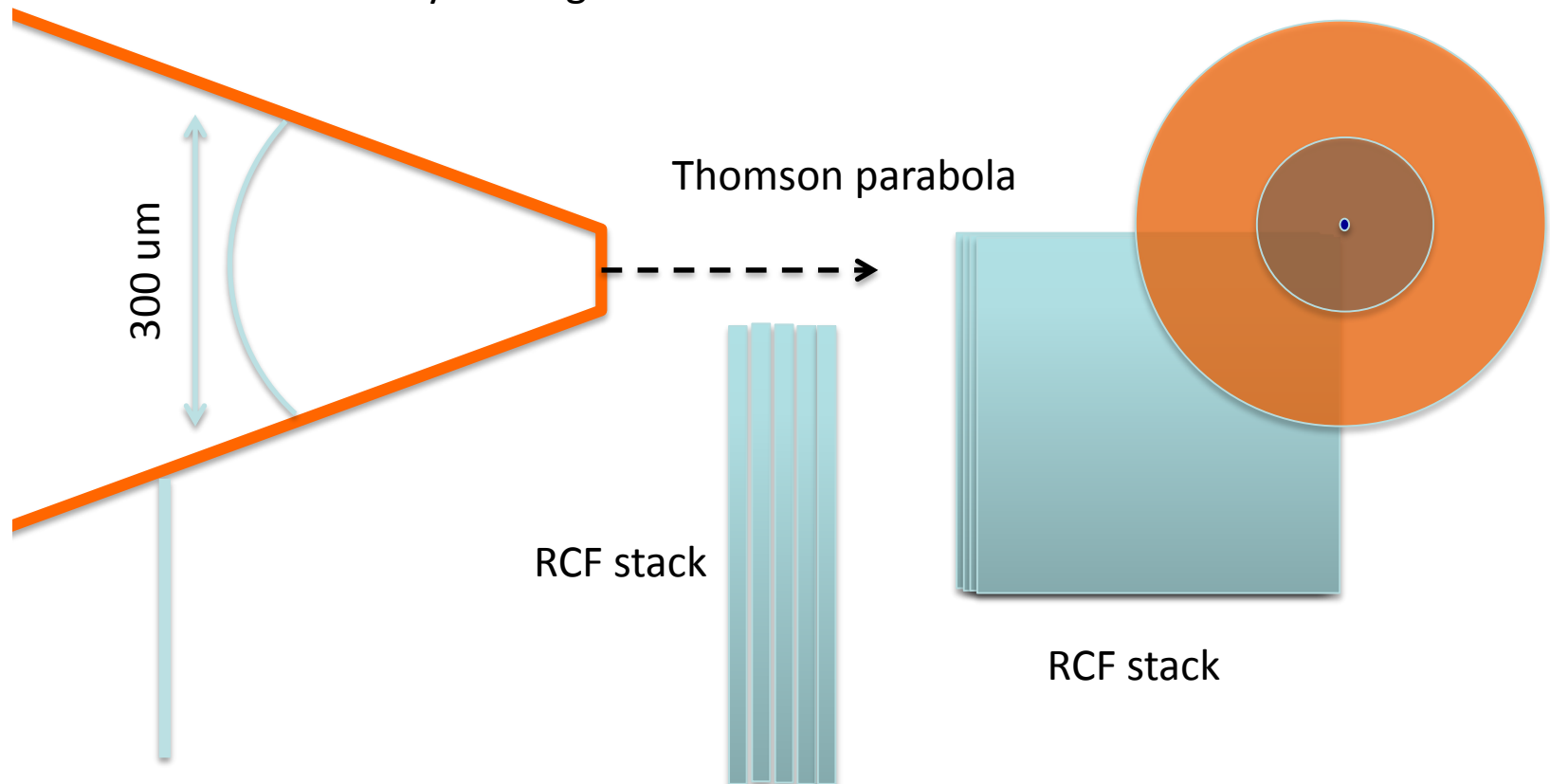
Experimental validation

Experiments carried out at ILE, Japan

- Free standing cone.

- Gold walls 15 μm thick.

- Hemispherical shell 350 μm radius.

- Pulse energy: 800 J.

- Pulse duration: 1.5 ps.

- Laser intensity on target ≈ 10^{19} Wcm^{-2}.

after A. Morace *et al.*

300 um

Thomson parabola

RCF stack

RCF stack

Confirmation of beam hollowing

The experimental results confirm the effect of B-fields on free standing cones with the protons being deflected in a ring-like shape by the B-fields
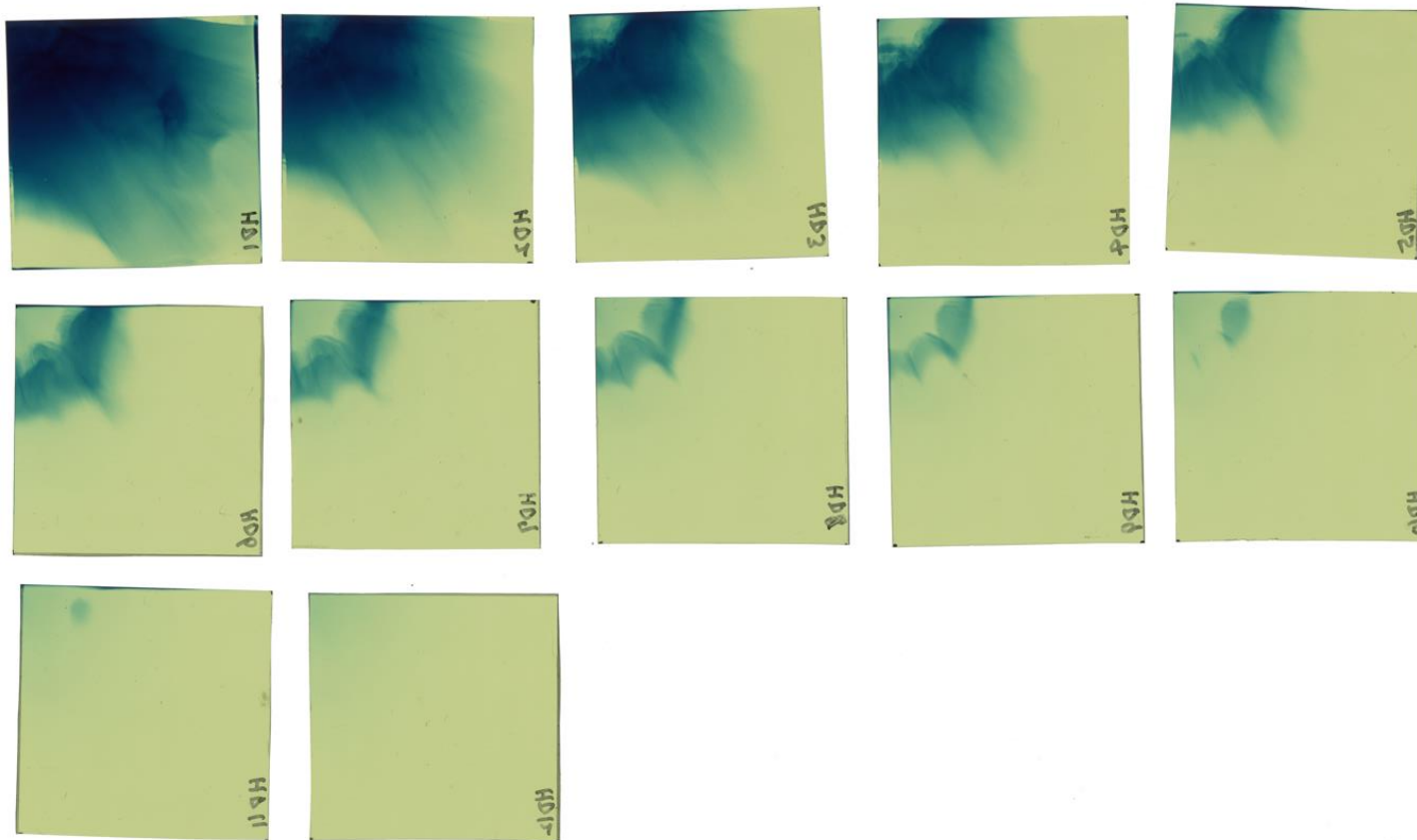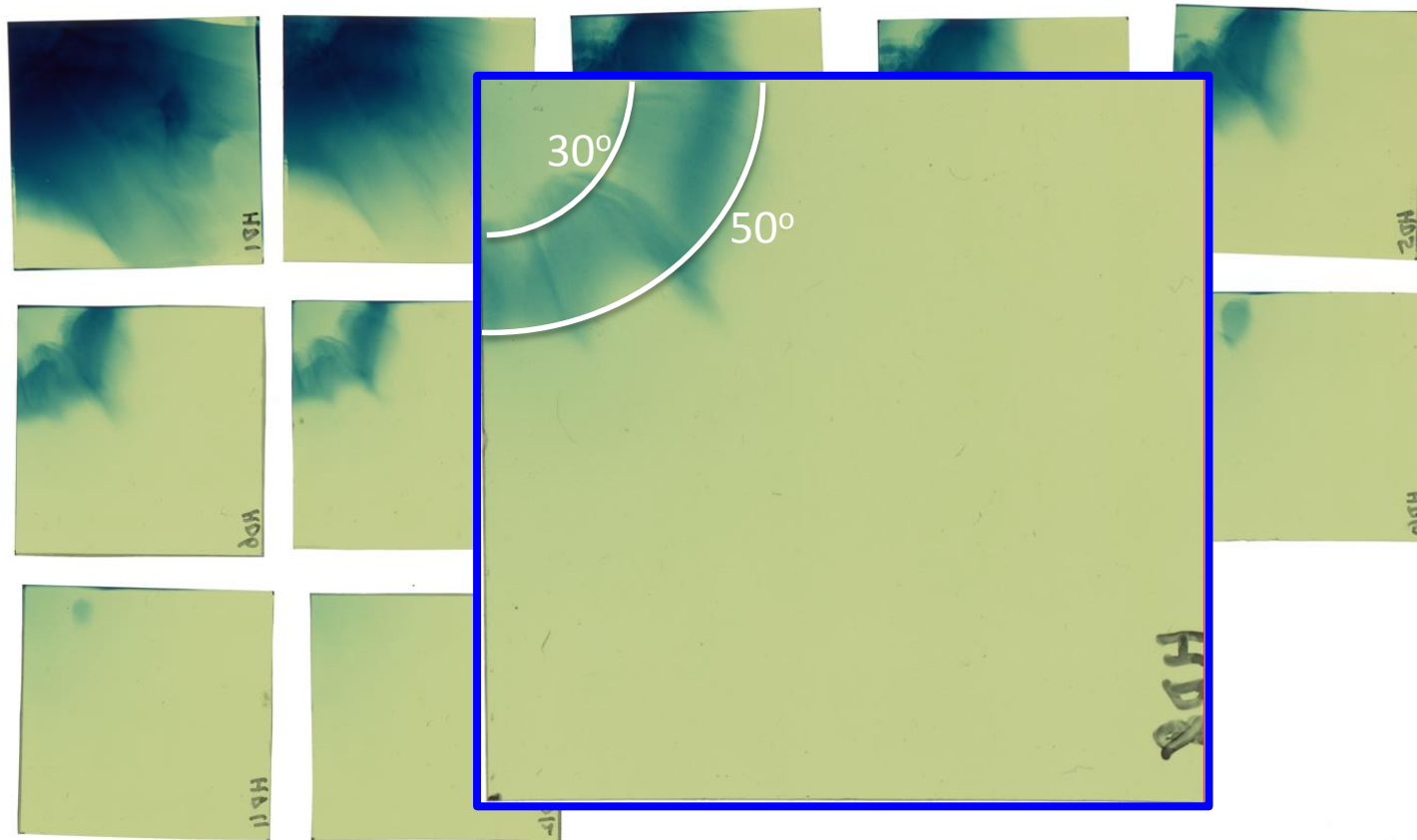
Confirmation of beam hollowing

The experimental results confirm the effect of B-fields on free standing cones with the protons being deflected in a ring-like shape by the B-fields

# New cone design to mitigate the B-fields near the cone walls

- Double cone with a '*second wall*' isolated from the laser-to-proton converter foil.

- No currents flow through the second wall because it is electrically isolated. Thus, the B-field is confined to the gap between the two cone walls.

- Only the B-field generated at the rear surface of the converter foil is dragged by the quasi-neutral plasma and amplified at the cone tip. This field is much lower than that generated by the surface currents,

Electron density

1.1×10^{23} cm^{-3}

Y [μm]

X [μm]
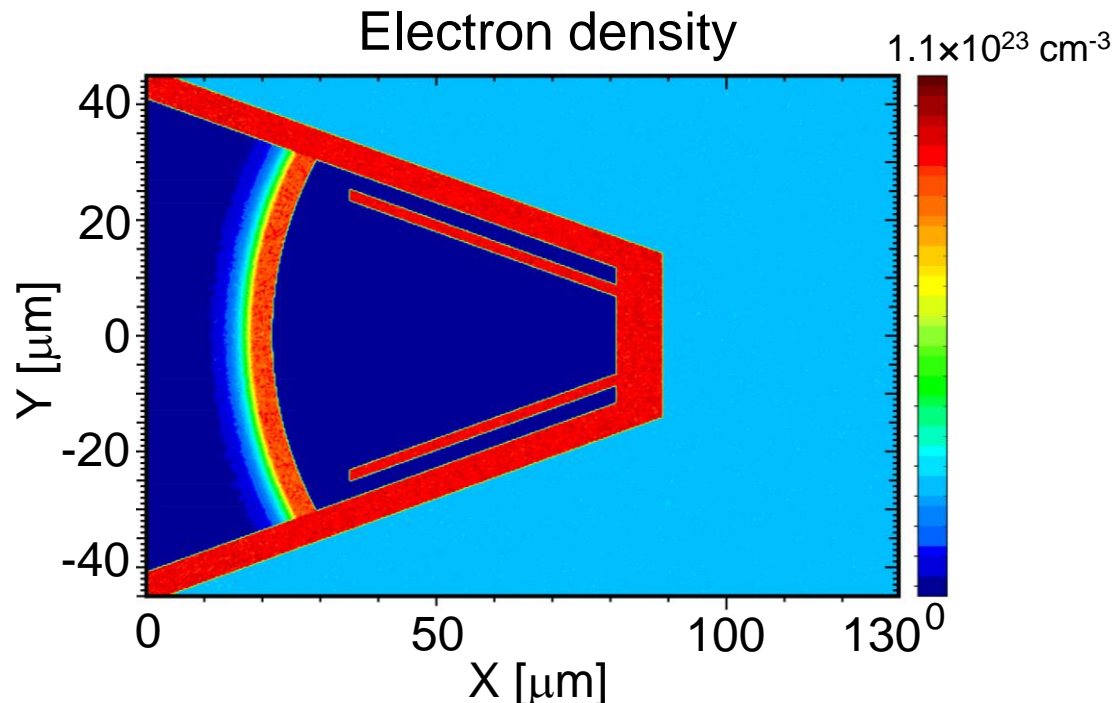
Double wall cone design to "shield" the quasi-neutral plasma from the B-field

- B-field generated by the currents flowing along the cone outer wall are 'confined' in the gap between the two walls.

- The B-fields at the cone tip are reduced substantially compared with the single wall cones. Even the low energy protons are well collimated.

- The divergence half-angle in this case is about 10 - 15° (HWHM) depending on the proton energy.

Laser intensity $I_{l,max}$ = 10^{20} W/cm^2, carbon cone tip .
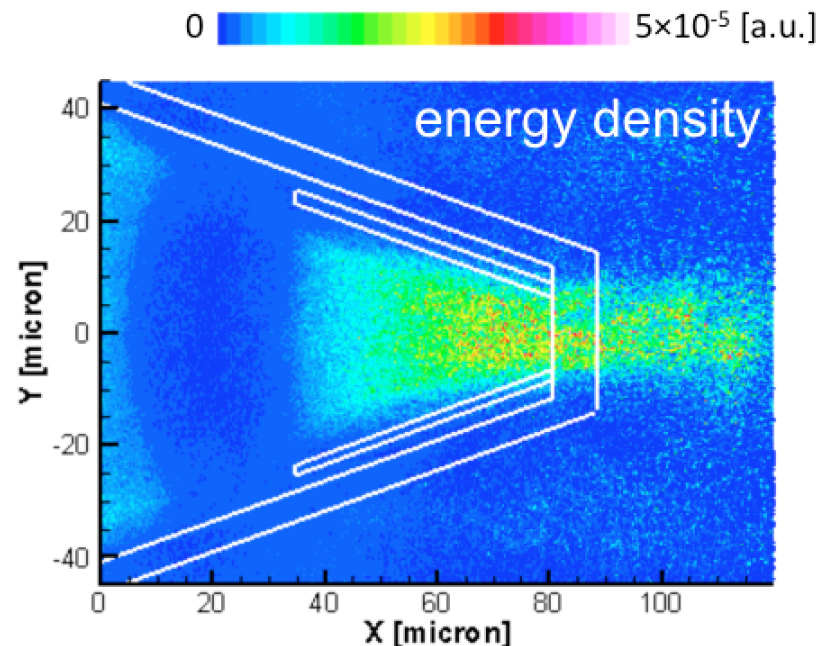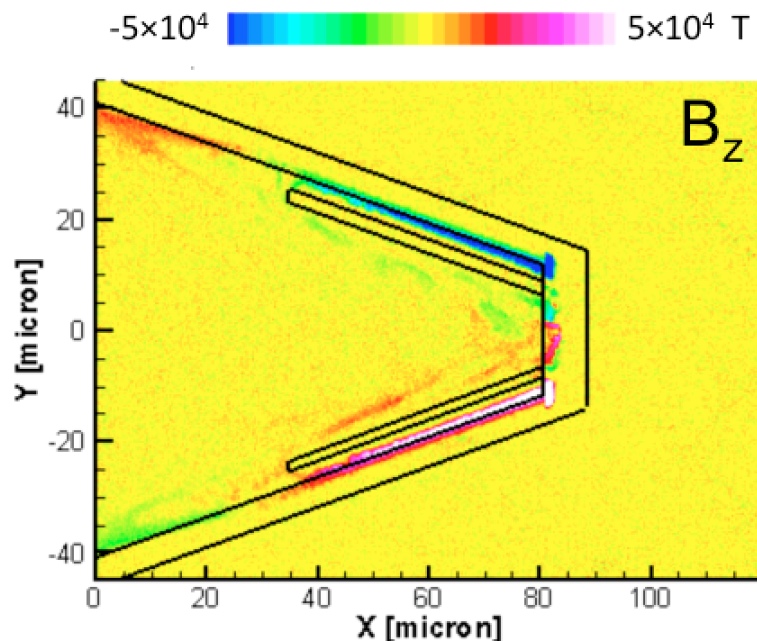
Summary

➢ PIC and hybrid simulations have proven to be very useful for experiment design and interpretation.

➢ *MareNostrum* and *Magerit* super-computers allowed us to carry out realistic simulations, competitive with those performed at the large scale laser facilities.

➢ We plan to study other alternative schemes to reduce the ignition energies. Some of those schemes are *shock ignition* and *magnetized inertial confinement fusion*.

➢ Those new schemes will be analyzed in close contact with experiments and within the context of the **EUROfusion** projects '***Towards inertial fusion energy***' and '***Preparation and Realization of European Shock Ignition Experiments***' funded by Euratom.

Thanks for your attention!